



HAL
open science

Some aspects of pulsed laser deposition of Si nanocrystalline films

B. Polyakov, A. Petruhins, J. Butikova, A. Kuzmin, I. Tale

► **To cite this version:**

B. Polyakov, A. Petruhins, J. Butikova, A. Kuzmin, I. Tale. Some aspects of pulsed laser deposition of Si nanocrystalline films. *European Physical Journal: Applied Physics*, 2009, 48 (2), pp.1-5. 10.1051/epjap/2009140 . hal-00518314

HAL Id: hal-00518314

<https://hal.science/hal-00518314>

Submitted on 17 Sep 2010

HAL is a multi-disciplinary open access archive for the deposit and dissemination of scientific research documents, whether they are published or not. The documents may come from teaching and research institutions in France or abroad, or from public or private research centers.

L'archive ouverte pluridisciplinaire **HAL**, est destinée au dépôt et à la diffusion de documents scientifiques de niveau recherche, publiés ou non, émanant des établissements d'enseignement et de recherche français ou étrangers, des laboratoires publics ou privés.

Some aspects of pulsed laser deposition of Si nanocrystalline films

B.Polyakov, A.Petruhins, J.Butikova, A.Kuzmin, I.Tale

Institute of Solid State Physics, University of Latvia,

Kengaraga st. 8, LV-1063, Riga, Latvia

Fax: (+371) 7132778, Phone: (+371) 26718631, E-mail: boris.polyakov@cfi.lu.lv

Abstract

Nanocrystalline silicon films were deposited by a picosecond laser ablation on different substrates in vacuum at room temperature. A nanocrystalline structure of the films was evidenced by atomic force microscopy (AFM), optical and Raman spectroscopies. A blue shift of the absorption edge was observed in optical absorption spectra, and a decrease of the optical phonon energy at the Brillouin zone centre was detected by Raman scattering. Early stages of nanocrystalline film formation on mica and HOPG substrates were studied by AFM. Mechanism of nanocrystal growth on substrate is discussed.

Keywords: Elemental semiconductors; Laser deposition; Thin films; Nanocrystalline materials

PACS numbers:

52.38.Mf Laser ablation

68.55.A Nucleation and growth

78.67.Bf Nanocrystals and nanoparticles

1. Introduction

Silicon is one of the most popular electronic materials as it is cheap and non-toxic, well and thoroughly studied. Besides silicon is highly attractive from the manufacturers' point of view. However, crystalline silicon (c-Si) has some drawback for solar cell applications: high price and low absorption coefficient in visible light spectrum. In contrast, nanocrystalline silicon (nc-Si) has some advanced features. It absorbs light better than c-Si, has less disordered structure than amorphous silicon (a-Si), and, hence, better electronic properties. Technology of nc-Si production is less demanding than c-Si technology and is very similar to a-Si technology [1], and may be easily adopted for mass production. Solar cells with the nc-Si layers were proved to be efficient and low-cost technology [2].

Among different deposition methods, pulsed laser deposition (PLD) is a simple and flexible technique for nanocrystalline film deposition. Si and Ge film deposited by PLD and films structure, electronic and optical properties were measured by number of groups [3, 4, 5]. However, it is still unclear whether nanocrystals are growing inside dense expanding plume or on the substrate surface in vacuum.

In this work, we present results of atomic force microscopy (AFM), optical absorption and Raman spectroscopies for nanocrystalline silicon films, prepared by picosecond laser ablation in vacuum.

2. Experimental

Ablation of single-crystal silicon rotating target proceeded at room temperature in vacuum 10^{-5} Torr, using third harmonic (355 nm) of Nd:YAG (SL-312, *EKSPLA*) 135 ps laser. Laser beam was focused into a spot of 1 mm in diameter. Several substrates were used: CaF₂ for optical measurements, highest quality mica and HOPG for AFM/Raman measurements.

Optical absorption spectra were measured on UV-VIS SPECORD spectrophotometer M40 (*Carl Zeiss*). Raman scattering spectra were measured on 3D scanning confocal microscope with spectrometer "Nanofinder-S" (Solar-TII). A HeCd laser (441.6 nm, 50 mW cw power) was used as a light source. The measurements were performed through Nikon CF Plan Apo 100x (NA=0.95) optical objective. The Raman spectra were recorded using 600 grooves/mm diffraction grating with a resolution of about 3-4 cm⁻¹ using the monochromator with 520 mm focal length and the edge filter to eliminate the elastic laser component. The power of the laser light at

the sample surface was controlled using variable neutral filter from 7 mW down to 0.5 mW, to exclude the possible influence of laser heating on the Raman signal [6]. No change in the Raman band position has been observed upon a variation of the laser power. Surface topography was measured by CP-II AFM (*Veeco*), tapping tips DP15 from Mikromasch were used.

The films thickness was obtained using the shadow mask method. TEM grid (the mask) was placed in a contact with the mica substrate during deposition process. After deposition the mask was removed, and the borders of Si islands, having rectangular shapes of about 24x24 μm , were scanned by AFM to measure resulting film thickness. The film thickness was about 20 nm after deposition during 30 min at laser pulse energy of 55 mJ that corresponds to the deposition rate 0.66 nm/min.

3. Results and discussion

Raman scattering spectra may be used to estimate a fraction of nanocrystalline and amorphous phases [7, 8]. Raman band at 480 cm^{-1} , associated with amorphous Si, is not present in our spectrum (Figure 1). It means that the film is mainly nanocrystalline. Due to the confinement effect in nanocrystals, the Brillouin zone centre optical mode, observed in the Raman spectrum of crystalline Si at $\sim 520\text{ cm}^{-1}$, shifts to smaller wave numbers and broadens [8]. Zi et al. describe the Raman shift for Si nanocrystals (NC) by the formula [9]:

$$\Delta\omega = -A(a/L)^\gamma, \quad (1)$$

where L is the diameter of a nanocrystal in \AA , $a = 5.431\text{ \AA}$ is the lattice constant of Si, $A = 47.41\text{ cm}^{-1}$ and $\gamma = 1.44$ are two parameters being due to the spherical shape of nanocrystals. Our measurements of Raman spectra show an average shift of about 12 cm^{-1} , that corresponds, according to the equation (1), to the average nanocrystals diameter of 15.3 \AA . Such nanocrystals are composed of about 90 silicon atoms [10].

According to our XRD results, the patterns of the films do not show any Bragg peaks and are thus x-ray amorphous. In the literature, the smallest Si nanocrystal size estimated by XRD measurements is $\sim 3\text{ nm}$ [11]. This means that the average nanocrystal size in our film is less than 3 nm.

Our optical absorption spectra (Figure 2a) are rather similar to that obtained by other researcher groups for nc-Si [4, 12]. The film thickness, measured by AFM, was used to calculate optical absorption coefficient.

Bulk Si is known as an indirect band gap material. However, some authors believe, that nanocrystalline Si is direct gap material [13]. Direct optical transitions are allowed in Si nanocrystals due to a quantum confinement [14], and the band gap shifts to higher energies. Oscillator strength strongly increases with decreasing atoms number in nanocrystal that, consequently, intensifies absorption [14]. Absorption coefficient α was fitted to experimental data in Figure 2 using two equations [15]:

$$\alpha \propto A \cdot (h\nu - E_g)^2 / h\nu \quad (2)$$

and

$$\alpha \propto A \cdot (h\nu - E_g)^{1/2} / h\nu, \quad (3)$$

where $h\nu$ is the photon energy and E_g is the band gap. The two equations describe absorption for indirect and direct band gap materials, respectively. Approximation of the optical absorption spectra by equation (2) gives $E_g \sim 2.15$ eV, whereas by equation (3) – $E_g \sim 3.25$ eV (Figure 2b,c). These values are larger than absorption edge of a-Si deposited in vacuum ($E_g \sim 1.2$ eV) and of a-Si annealed at 400° C ($E_g \sim 1.4$ eV) [16]. Unfortunately, we cannot measure optical losses of reflected and scattered light, that leads to an error in E_g estimation due to the background (Figure 2b). Reflection at silicon surface at 1.4 eV is about 31% [17].

Note that the direct band gap model, equation (3), gives better fit to experimental data (Figure 2b,c) in our case. At the same time, Wilcoxon et al. have concluded on the indirect band gap for 18 Å Si nanocrystals [12]. In his work the optical absorption in Si nanocrystals, having very narrow size distribution, was explained in terms of indirect band gap model (absorption edge blue shifted to 2.2 eV by quantum confinement), and characteristic features of nc-Si absorption spectrum were identified with transitions in bulk Si (direct optical transition at 3.5 eV). In our case, nanocrystals have rather broad distribution, and we believe that indirect and direct absorption are mixed up in the spectra (Figure 2b, c). Consequently, optical band gap of our nanocrystalline film, averaged over size distribution of nanocrystals, is about 2.15 eV. In literature band gap values of Si nanocrystals of similar size are in the range 2.0-3.5 eV [12].

To visualize the early stage of film formation, we deposited Si on mica and HOPG during 30 s and 120 s, corresponding to 300 and 1200 laser shots, respectively. According to the deposition speed at given laser intensity, we should deposit about 0.33 and 1.32 nm of Si material, respectively. We expected two possible scenarios of

nanocrystal deposition on substrate (Figure 3 a,b and c,d). Nanocrystals of diameter d_1 , which grow in plume during the flight, land on the substrate and their amount is a linear function of time. At t_1 (30 s) number of nanocrystals is small, and there are more nanocrystals at $t_2 > t_1$ ($t_2 = 120$ s), but their diameter d_1 does not change (Figure 3 a,b). In the second scenario, nanocrystals grow on substrate surface, initially their diameters $d_2 \ll d_1$ at t_1 , and it increase with time up to d_2' at t_2 (Figure 3 c,d).

On mica substrate, we found surprisingly little amount of Si nanoparticles after deposition during 120 s of deposition on $3 \times 3 \mu\text{m}^2$ area and almost nothing after 30 s. Using HOPG as a substrate, it was possible to observe surface modifications after 30 s (Figure 4a, b). A large number of nanoparticles were found after deposition during 120 s. Small particles were counted on an area of $600 \times 600 \text{ nm}^2$, whereas large particles were counted on an area of $2.5 \times 2.5 \mu\text{m}^2$. The resulting histograms are presented in the Figure 5a and b. We note that nanoparticles, having a size of 0-1 nm could not be counted correctly on area of $600 \times 600 \text{ nm}^2$ and they were not included into the first histogram. Due to the same reason, nanoparticles having a size of 0-5 nm were not included into the second histogram.

Bulgakov et al. [18] has showed that the most abundant species produced by femtosecond laser are Si^+ cations and Si neutral atoms, with a small number of Si_n^+ and Si_n clusters, those amount decreases rapidly upon increasing n. We used a permanent magnet to bend the trajectory of Si species produced by laser ablation. Most particles were focused by magnetic field (Figure 6): this means that most of them are small charged particles, probably Si^+ cations or Si_n^+ clusters with very small n, dimers or trimers. According to [18], Si species with high kinetic energy are more forward directed than slow ones. We found that optical absorption spectra measured on film deposited apart from plume axis (6 mm in our case), have increased absorption at low photon energy visible till 2.7 eV (Figure 2a): we attribute this absorption to dangling bonds of Si atoms [2].

Properties of our nanocrystalline films are close to that produced by Wu et al [4]. However, in contrast to [4], we believe that the growth of nanocrystals happens not in the plume, when ejected Si species fly from the target, but after their landing onto the substrate. In the paper by van Buuren et al. [19], thermally evaporated Si atoms build nanocrystals with the average size of 2.4 nm and the band gap E_g of 2.3

eV. It was also found [19] that nanocrystals are mobile on HOPG and form snowflakes like super clusters.

Flying Si particles, produced by laser ablation, have rather high kinetic energy of about 20 eV [18]. After landing they may diffuse over the surface and build nanocrystals. Activation energy for a diffusion of Si atoms over Si surface is in the range of 0.08-1.6 eV [20, 21]. Taking into account the results of optical absorption spectra, Raman scattering and AFM data, we conclude that ablated Si species tend to build nanocrystals with the average size of about 15 Å.

4. Summary

According to the optical absorption and Raman scattering spectra, a film deposited by PLD in vacuum is nanocrystalline with the average nanocrystal size of 15 Å and the band gap $E_g = 2.15$ eV. AFM studies of nanocrystals on HOPG and trajectory bending of flying Si species by magnetic field suggest that the majority of nanocrystals grow on substrate surface fed by energetic Si^+ supplied from the plume.

Acknowledgments

The authors are grateful to Dr. J.Maniks, Dr. L.Grigorjeva, Dr. E.Tamanis and Dr. P.Kulis for help and assistance during experiments. This study was supported by the European Social Fund.

References

1. M. Esmaili-Rad, A. Sazonov, A. Kazanskii, A. Khomich, A. Nathan, J. Mater. Sci: Mater Electron. **18**, S405 (2007)
2. A. Shah, J. Meier, E. Vallat-Sauvain, C. Droz, U. Kroll, N. Wyrsh, J. Guillet, U. Graf, Thin Solid Films. **403–404**, 179 (2002)
3. L. Patrone, D. Nelson, V. Safarov, S. Giorgio, M. Sentis, W. Marine, Appl. Phys. A. **69**, S217 (1999)
4. M. Wu, R. Mu, A. Ueda, D. Henderson, B. Vlahovic, Mater. Sci. Eng. B. **116**, 273 (2005)
5. D. Riabinina, F. Rosel, M. Chaker, J. Exp. Nanosci. **1**, 1, 83 (2005)
6. S. Piscanec, M. Cantoro, A. C. Ferrari, J. A. Zapien, Y. Lifshitz, S. T. Lee, S. Hofmann, J. Robertson, Phys. Rev. B **68**, 241312 (2003)

7. R. Tsu, J. Gonzalez-Hernandez, S. Chao, S. Lee, K. Tanaka, Appl. Phys. Lett. **40**, 6, 534 (1982)
8. G. Viera, S. Huet, L. Boufendi, J. Appl. Phys. **90**, 8 (2001)
9. J. Zi, H. Buscher, C. Falter, W. Ludwig, K. Zhang, X. Xie, Appl. Phys. Lett. **69**, 2 (1996)
10. A. Zunger, L.-W. Wang, Appl. Surf. Sci. **102**, 350 (1996)
11. T. Torchynska, A. Vazquez, G. Polupan, Y. Matsumoto, L. Khomenkova, L. Shcherbyna, J. Non-Cryst. Sol. **354**, 2186 (2008)
12. J. Wilcoxon, G. Samara, P. Provencio, Phys. Rev. B. **60**, 4, 15, 2704 (1999)
13. T. Mohantya, N. Mishrab, A. Pradhanc, D. Kanjilala, Surf. Coat. Technol. **196**, 34 (2005)
14. B. Delly, E. Steigmeier, Phys. Rev. B. **47**, 3, 1397 (1993)
15. P. Yu, M. Cardona, *Fundamentals of Semiconductors*, 3rd edn. (Springer, 2002)
16. M. Brodsky, R. Title, K. Weiser, G. Petit, Phys Rev. B. **1**, 6, 2632 (1970)
17. J. Chelikowsky, M. Cohen, Phys. Rev. B. **14**, 2, 556 (1976)
18. A. Bulgakov, I. Ozerov, W. Marine, Thin Solid Films, **453–454**, 557 (2004)
19. T. van Buuren, L. Dinh, L. Chase, W. Siekhaus, L. Terminello, Phys. Rev. Lett. **80**, 17, 3803 (1998)
20. G. Brocks, P. Kelly, Phys Rev. Lett.. **66**, 13, 2498 (1991)
21. Y. Mo, J. Kleiner, M. Webb, M. Lagally, Phys Rev. Lett. **66**, 15, 1729 (1991)

Figure captions

Figure 1. Raman spectrum of nanocrystalline PLD nc-Si film and single-crystal c-Si in the region of the $k=0$ optical mode.

Figure 2. Absorption spectra of PLD Si film on CaF_2 (a), and two different fitting of absorption spectra (b and c).

Figure 3. Simplified schematics of possible Si NC deposition.

Figure 4. AFM images of clear HOPG surface (a), Si NC deposited on HOPG for 30 s (b) and 120 s (c). Scan size $600 \times 600 \text{ nm}^2$.

Figure 5. Histograms of Si NC size distribution on HOPG deposited for 120 s for $600 \times 600 \text{ nm}^2$ (a) and $2.5 \times 2.5 \text{ }\mu\text{m}^2$ (b).

Figure 6. Bending of ablated Si atoms trajectory using magnet: (a) scheme of deposition through the diaphragm; (b) scheme of deposition through the magnet, hole in magnet is equal to diaphragm hole; (c) photograph of the magnet; (d) photograph of a sample coated with Si through the diaphragm, (e) photograph of a sample coated with Si through the magnet.

Figures

Figure 1.

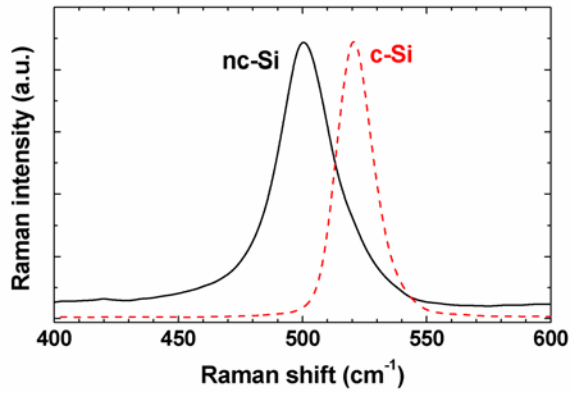


Figure 2.

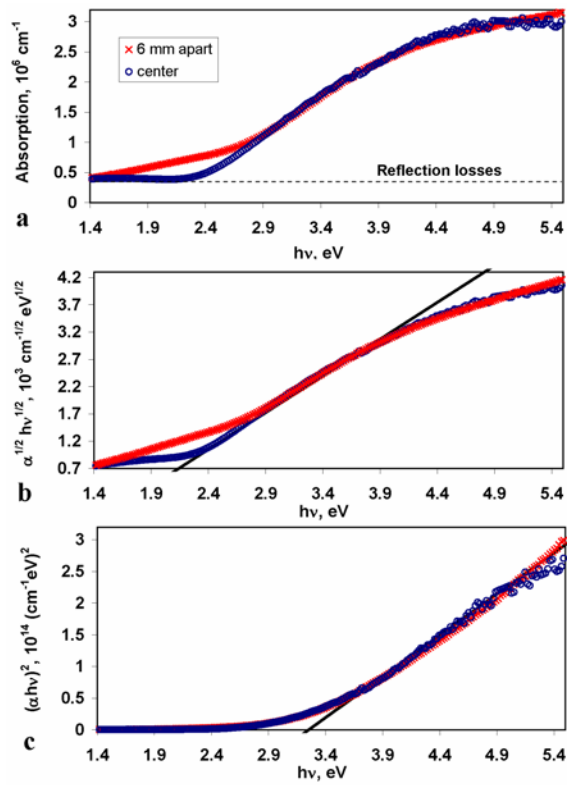


Figure 3.

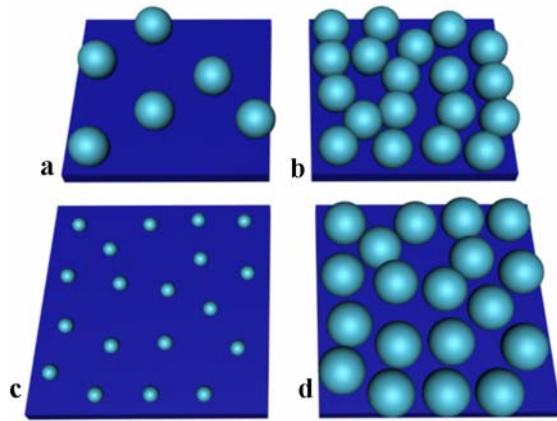


Figure 4.

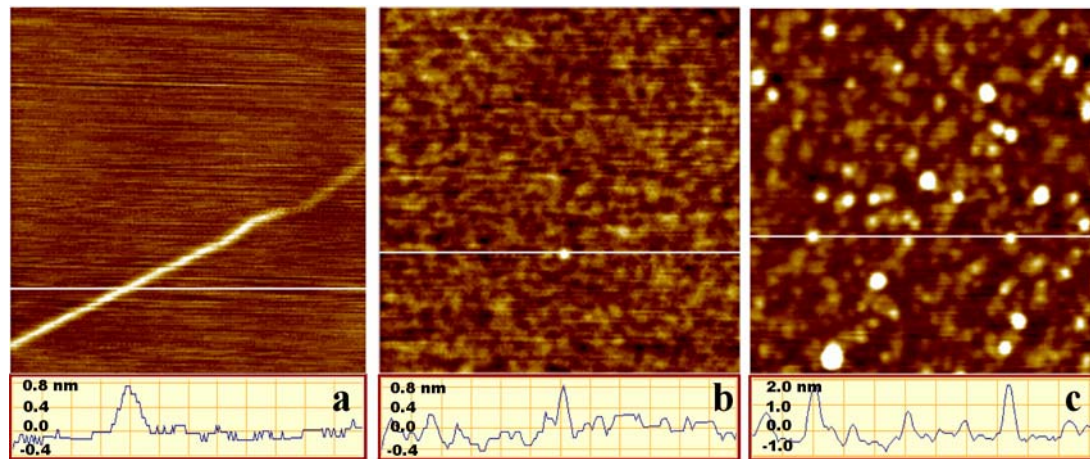


Figure 5.

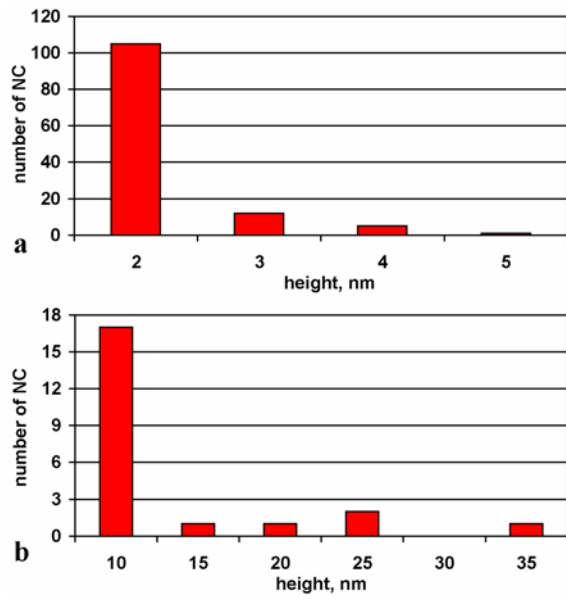


Figure 6.

